

Dynamics of intrinsic and nitrogen-induced exciton emission in indirect-gap $\text{Ga}_{1-x}\text{Al}_x\text{As}$

M. D. Sturge, E. Cohen,* and R. A. Logan

Bell Laboratories, Murray Hill, New Jersey 07974

(Received 30 July 1982)

We report measurements of low-temperature luminescence spectra, lifetime, and excitation spectra for excitons in $\text{Ga}_{1-x}\text{Al}_x\text{As}$ ($x_c < x < 0.55$, where $x_c = 0.435$ is the direct-to-indirect crossover value) over a wide range of excitation levels. The no-phonon line, ~ 6 meV wide, decays nonexponentially at low excitation levels. The decay rate depends strongly on excitation intensity and on temperature (for $2 < T < 30$ K) while the position and width remain unchanged. We show that in the low-temperature, low-excitation limit, the nonexponential decay, and its dependence on x , can be quantitatively explained in terms of emission from a small number of localized indirect excitons scattered by alloy fluctuations. Above 8 K these excitons become mobile and their decay is exponential. Most of the excitons are mobile even at 2 K. They dominate the emission when the excitation is sufficiently strong to neutralize the ionized impurities, which quench the luminescence at low intensities. The localized excitons show strong LO-phonon sidebands, while the mobile ones do not. The theory of the decay rate yields a mean value of the scattering strength $J \sim 0.2$ eV, in reasonable agreement with estimates from the Al-Ga electronegativity difference. The nitrogen-bound exciton with a wide range of binding energies, previously reported in ion-implanted samples, is found to be split, possibly by a disorder-induced axial field.

I. INTRODUCTION

The low-temperature luminescence of nominally pure indirect-gap compound semiconductors is concentrated just below the band gap and is usually dominated by the radiative decay of excitons bound to residual impurities.¹ There are two reasons for this extrinsic behavior: (1) No-phonon decay of free excitons is forbidden by the conservation of momentum; (2) free excitons are rapidly captured by the impurities which are present at the 10^{15} – 10^{16} - cm^{-3} level in even the best available material.

In alloy semiconductors both conditions are somewhat relaxed by the intrinsic fluctuations in potential, due to the alloy disorder, which scatter excitons. The large k components of the fluctuating potential break the \vec{k} -selection rule and make no-phonon transitions allowed.² The long-range (small k) components inhibit the migration of "free" excitons to impurity centers and may even be strong enough to form a bound state of the exciton.³

Indirect-exciton absorption induced by the potential fluctuations in an alloy semiconductor was first observed by Dean *et al.*⁴ in $\text{GaAs}_{0.07}\text{P}_{0.93}$. Subsequent work on this induced absorption is reviewed by Pikhtin.² He points out that, because of impurity effects, the influence of alloy fluctuations on indirect exciton emission is difficult to establish.

Lai and Klein⁵ have reported an emission line in

indirect-gap $\text{GaAs}_{1-x}\text{P}_x$ which they attribute to excitons bound by potential fluctuations. The density of bound states is very low ($\sim 10^{15}$ cm^{-3}), and in consequence it is difficult to rule out the possibility that the center is some unknown impurity or defect.

Apart from this unique case, all emission within a few meV of the band gap in such alloy semiconductors as $\text{GaAs}_{1-x}\text{P}_x$,^{6,7} $\text{In}_{1-x}\text{Ga}_x\text{P}$,^{8,9} and $\text{Ga}_{1-x}\text{Al}_x\text{As}$ (Refs. 10–13) has in the past been attributed to excitons bound to impurities, usually donors or the isoelectronic trap N.¹³ However, the correctness of this attribution in undoped material has not always been firmly established.

We report here low-temperature measurements of luminescent lifetime and excitation spectra in nominally undoped $\text{Ga}_{1-x}\text{Al}_x\text{As}$ with $x_c < x \leq 0.55$, where $x_c = 0.435$ is the value of x at which the Γ and X conduction minima cross.¹⁴ Our measurements were made at excitation levels up to the threshold for the formation of an electron-hole plasma,¹⁵ (i.e., $\sim 10^{18}$ cm^{-3} , more than enough to saturate any impurity levels). We find a strong no-phonon line whose position and width is independent of excitation level, but whose lifetime increases with excitation level to a value much greater than that observed in deliberately doped crystals. Analysis of the dependence of the lifetime on x near x_c shows that the scattering centers responsible for breaking the \vec{k} -selection rule have such a high densi-

ty ($> 10^{19} \text{ cm}^{-3}$) that they can only be the intrinsic alloy fluctuations. At very low excitation level, the decay is nonexponential and can be quantitatively accounted for only by taking into account the exponential distribution of scattering probabilities¹⁶ for localized excitons.

We give the results of this work on undoped $\text{Ga}_{1-x}\text{Al}_x\text{As}$ in Sec. III, and show how they demonstrate the intrinsic nature of the exciton in Sec. IV. In Sec. V we report and discuss some curious new results obtained on the exciton bound to nitrogen.

II. EXPERIMENTAL PROCEDURE

We used $\text{Ga}_{1-x}\text{Al}_x\text{As}$ epilayers, 5–10 μm thick, grown on GaAs substrates by liquid-phase epitaxy. The net donor concentration in nominally undoped samples, measured by Schottky barrier capacitance, was in the range $1\text{--}3 \times 10^{16} \text{ cm}^{-3}$. Some samples were grown with $1\text{--}3 \times 10^{-3} \text{ NH}_3$ in the ambient, but comparison with data on ion-implanted samples shows that in only one case, to be discussed in Sec. V, was appreciable nitrogen doping achieved.

In order to determine the Al-Ga ratio the GaAs substrate was etched away and the absorption spectrum obtained. This gives the direct gap E_{Γ} , from which we obtained the composition parameter x , using the calibration of Dingle *et al.*¹⁴ Because x increases through the depth of the layer by about 0.005 per micrometer,¹⁷ the Γ exciton peak is not observed in the absorption spectrum of a "thick" ($\geq 4 \mu\text{m}$) layer. To obtain a more precise value of x at the front surface we used the luminescent excitation spectra, which do show a well-resolved exciton peak, whose position agrees well with the onset of absorption.

Both cw and pulsed photoluminescence was studied. For cw spectroscopy a tunable dye laser pumped by an Ar^+ laser was used. In most cw experiments the average intensity at the sample surface did not exceed 1 W/cm^2 . The dye-laser linewidth was 0.3 \AA . For intense excitation a tunable dye laser pumped by a pulsed N_2 laser was used. The peak power was 1–10 kW, the repetition rate 50 Hz, and the pulse width 5 nsec at half maximum. The peak excitation intensity at the samples surface was varied between 10^3 and 10^7 W/cm^2 . The laser linewidth was less than 0.1 \AA . The photoluminescence was monitored with a double monochromator (resolution 0.1 \AA) equipped with a cooled photomultiplier which had a rise time of 2 nsec. The pulses were analyzed with a boxcar integrator with a gatewidth down to 1 nsec.

Some lifetime measurements were also made at a lower excitation level, $\sim 1\text{--}100 \text{ W/cm}^2$, by the time-resolved photon-counting technique. The

source was a cw laser, whose output was chopped with an acoustic-optic modulator. This system has a repetition rate of up to 1 MHz and a time resolution of 15 nsec.

The samples were either immersed in liquid helium (for 2 and 4.2 K runs) or mounted in a temperature-controlled flow-through cryostat (for $T > 4.2 \text{ K}$). In the latter case the samples were in contact with the cold helium gas in order to provide heat dissipation from the illuminated surface. The temperature was stabilized to better than 0.2 K and the temperature of the crystal mount was monitored with an accuracy of 0.1 K. At high-excitation levels, the actual crystal temperature was up to 2 K higher than measured due to heating by the photoexcitation.

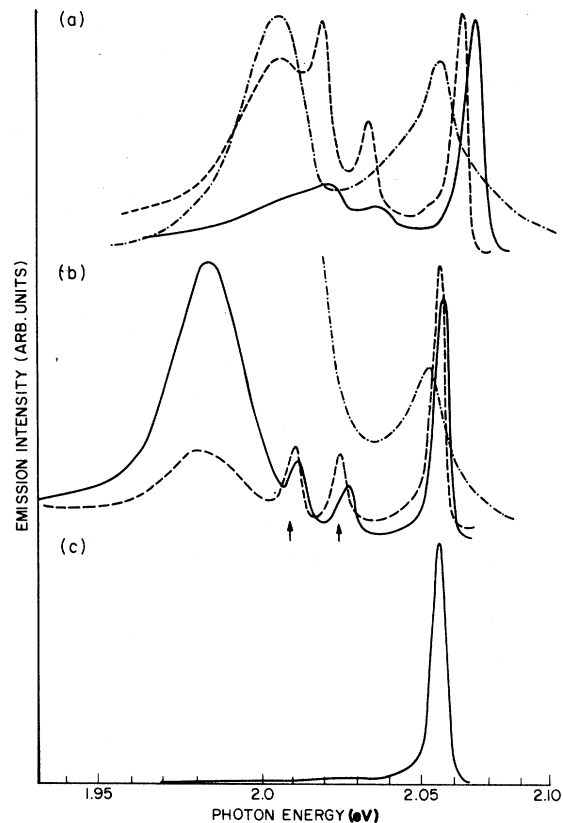


FIG. 1. Emission spectra of $\text{Ga}_{1-x}\text{Al}_x\text{As}$ at 2 K under the cw and pulsed excitation (a) $x=0.52$, cw; (b) $x=0.46$, cw; (c) $x=0.46$, pulsed. The solid line represents the undoped crystal, the dashed line a crystal grown in NH_3 ambient, and the dotted-dashed line a Te doped crystal (measured at 4.4 K). The arrows in (b) indicate the expected positions of $\vec{k}=0$ LO-phonon sidebands for the undoped crystal (solid line).

III. RESULTS

A. Low-temperature spectra

Figure 1 shows the near band-gap cw emission spectra at 2 K of $\text{Ga}_{1-x}\text{Al}_x\text{As}$ with $x=0.46$ and 0.515. The liquid-phase epitaxial (LPE) layers were either undoped, doped with Te, or grown in an NH_3 ambient in an attempt to dope with N. Samples doped with Sn gave spectra identical to those for Te.

The main features of these spectra are as follows. There is a relatively sharp [full width at half maximum (FWHM) ~ 6 meV] no-phonon line peaking at 2.06 eV for $x=0.515$ and at 2.055 eV for $x=0.46$, which we attribute to the decay of indirect (X) excitons. Its position is shown, as a function of x and of doping, by the points of Fig. 2. The broad feature peaking near 1.97 eV has the long lifetime and characteristic saturation behavior of a donor-acceptor (DA) pair band, and will not be discussed further. Riding on this band are two phonon sidebands of the exciton line. Their energy shifts are 31 ± 1 and 46 ± 1 meV, slightly less than the known energies of the two $\vec{k}=0$ LO phonons of $\text{Ga}_{1-x}\text{Al}_x\text{As}$, which is a two-mode system.¹⁸ These two bands were reported by Dingle *et al.*¹² who attributed them to transitions made allowed by momentum-conserving X -point LO phonons, which were assumed to coincide approximately in energy

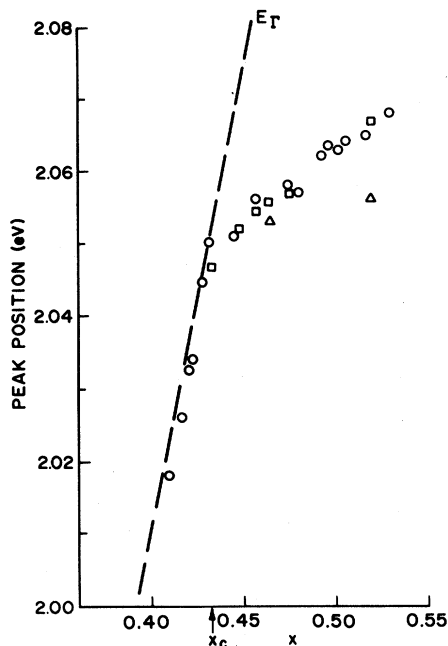


FIG. 2. Observed positions of no-phonon emission lines of $\text{Ga}_{1-x}\text{Al}_x\text{As}$ at 2 K as a function of composition and doping, where \circ undoped; \square grown in NH_3 ; and \triangle Te- or Sn-doped.

with the $\vec{k}=0$ phonons. The phonon sidebands are quite weak and their integrated intensity, relative to the no-phonon line, depends on doping, on excitation intensity and wavelength, and on temperature.

A typical spectrum obtained with pulsed excitation is shown in Fig. 1(c). Pulse-excited spectra were obtained with a short (~ 10 nsec) gate, so it is not surprising that the long-lived DA luminescence is suppressed. What is more surprising is that the phonon sidebands of the exciton emission have also disappeared. The no-phonon line is almost identical, in position and line shape, to that obtained under cw excitation.

The intensity I of the no-phonon luminescence varies nonlinearly with excitation intensity I_{ex} . The relative radiative efficiency, I/I_{ex} , for $x=0.46$, is plotted as a function of I_{ex} in Fig. 3. These data were obtained with pulsed (solid line) and cw (dashed line) excitation. The cw data for the phonon sideband are also shown (dotted-dashed line). The vertical scales for the no-phonon line have been arbitrarily matched at the peak. The horizontal scales have been matched to nominally equal excitation density on the basis of the observed average lifetime of about 100 nsec. Note the strongly superlinear behavior at low I_{ex} . The sublinearity at high I_{ex} is associated with the formation of the electron-hole plasma, as has been discussed elsewhere.¹⁵

The superlinear behavior implies that nonradiative decay paths are becoming saturated. Under pulsed excitation the saturation intensity is of order 3×10^{12} photons $\text{cm}^{-2}/\text{pulse}$, or 3×10^{16} $e-h$ pairs cm^{-3} . Comparison with the cw saturation curve shows that the saturating nonradiative centers have lifetimes predominantly in the range 1 to 10 μsec . This is the range expected for DA pairs in this quasidirect material. It is too long for deep recombination centers which decay by multiphonon emission, or for shallow neutral donors or acceptors which bind excitons and decay rapidly by Auger emission. It is also too long for an isoelectronic center such as nitrogen, an exciton bound to which has a lifetime in the range of nanoseconds (see Sec. V). The density at which saturation occurs, $\sim 3 \times 10^{16}$ cm^{-3} , is also consistent with the estimated shallow impurity content of these compensated samples. Since ionized impurities produce local electric fields which are sufficiently strong to destroy the exciton, it is not surprising that they dominate its nonradiative decay. Of course this process is not strictly nonradiative, since most of the energy subsequently emerges radiatively as DA pair luminescence, which we observe. However, from the point of view of exciton luminescence it is the predominant loss mechanism at low-excitation level, and will be referred to as nonradiative in this paper.

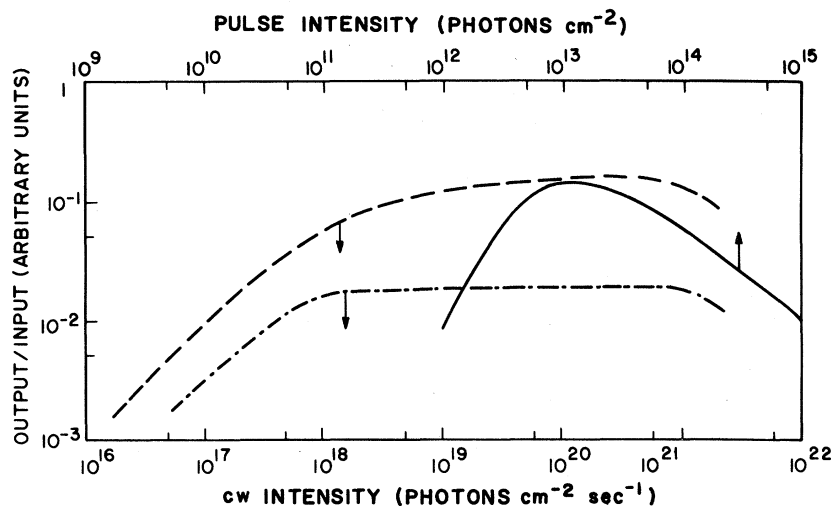


FIG. 3. Dependence on excitation intensity of the relative radiative efficiency for $x=0.46$ at 2 K; — no phonon line, pulsed excitation; --- no-phonon line, cw; -·-·- phonon sideband, cw.

B. Temperature dependence

Under cw excitation the exciton line weakens rapidly as the temperature is raised, and it is not visible above 20 K. If this decrease in intensity is ascribed to a temperature-dependent nonradiative decay rate w_{NR} , we can write¹⁹

$$y(T) = \frac{I(0)}{I(T)} - 1 = \frac{w'_{NR}(T)}{w_r + w_{NR}(0)}, \quad (1)$$

where w_r is the mean radiative decay rate, and

$$w'_{NR}(T) = w_{NR}(T) - w_{NR}(0).$$

The circles in Fig. 4 show an Arrhenius plot of $y(T)$ for the integrated no-phonon intensity of an undoped sample with $x=0.46$. The results show two activation energies for w'_{NR} , 5.5 and 21 meV. The latter can be attributed to dissociation of the exciton into free particles, since the free indirect exciton has a binding energy of about 20 meV. The origin of the 5.5-meV activation energy has no such obvious interpretation.

A clue to its origin is given by the observation that the no-phonon line shifts to lower energy as temperature increases. This shift is much greater than the expected shift of the band gap (less than 0.5 meV from 0 to 25 K in the analogous case²⁰ of GaP). It implies an activation energy E_a which depends on emission energy $h\nu$. The actual (not integrated) intensity data for an emission energy just below and just above the peak of the no-phonon line have been substituted in Eq. (1) and the results are plotted in Fig. 4 (squares and triangles, respectively). While these data are less precise than the integrated intensity data, since they do not allow for the line broadening with temperature, they do indicate an in-

creasing E_a with decreasing $h\nu$ (i.e., with increasing depth of the potential well in which the exciton lies). Note, however, that the change in E_a , is less, by a factor of 2, than the change in $h\nu$.

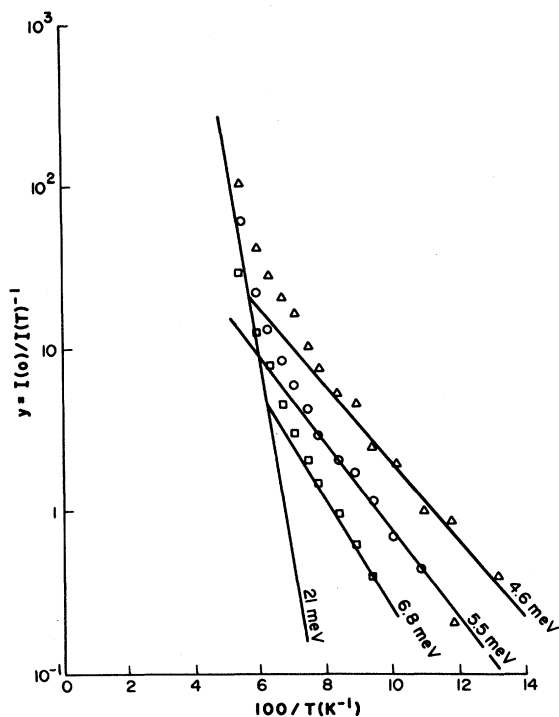


FIG. 4. Temperature dependence of the emission intensity $I(T)$ under weak cw excitation (about 10^{18} photons $\text{cm}^{-2} \text{sec}^{-1}$), plotted as $y(T) = I(0)/I(T) - 1$ against T^{-1} . \circ , $I(T)$ is the integrated intensity of no-phonon line; \square , $I(T)$ is the intensity at 2.051 eV, and \triangle , $I(T)$ is the intensity at 2.0575 eV. The lines have the activation energies indicated.

C. Time-dependent measurements

A series of time-resolved spectra for $x=0.445$, $T=2$ K, obtained at low-excitation intensity, are shown in Fig. 5. In this sample the no-phonon line sharpens somewhat with time, but, as in other samples, the peak does not shift. The phonon sidebands, very weak at zero delay, decay at a slower rate than the no-phonon line.

The 2 K decay curve for the peak of the no-phonon line at $x=0.46$, after excitation with a short, weak pulse, is shown in Fig. 6. Similar curves for other x are shown in Ref. 16. Note the nonexponential behavior. It has been shown,¹⁶ as is discussed in the next section, that if alloy scattering is responsible for the no-phonon line, while the sideband is induced by momentum-conserving (MC) X -point phonons, the decay of localized excitons after a short pulse should follow

$$\frac{I(t)}{I(0)} = \frac{e^{-w_1 t}}{(1 + w_m t)^2} \quad (\text{no-phonon-line}) \quad (2)$$

or

$$\frac{I(t)}{I(0)} = \frac{e^{-w_1 t}}{(1 + w_m t)} \quad (\text{sideband}). \quad (3)$$

Here w_m is the average radiative decay rate due to alloy scattering, and w_1 is the total decay rate due to all other processes. The no-phonon data fit Eq. (2) well, as illustrated in Fig. 6, showing that at this low excitation level and temperature the excitons are localized on the time scale of the radiative lifetime. It is difficult to measure the phonon sidebands accurately at long delay, because of the underlying donor-acceptor recombination, but they do not appear to follow either Eq. (2) or (3) very precisely.

Raising the temperature above 8 K produces a ra-

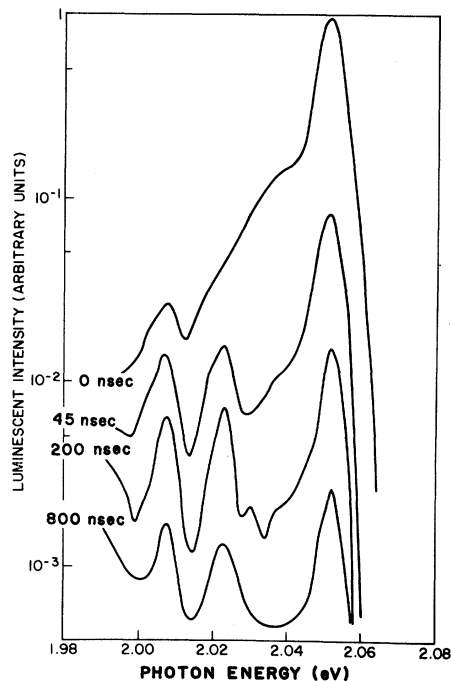


FIG. 5. Time-resolved emission spectra for $x=0.445$, $T=2$ K. Excitation is by a 10-nsec pulse at 5145 \AA , $\sim 10^{12} \text{ photons cm}^{-2} \text{ pulse}^{-1}$. Gatewidth is equal to 50% of delay (minimum 10 nsec).

pid changeover to exponential decay, as shown in Fig. 7. There is a concomitant decrease in radiative efficiency η . If we take η to be unity below 8 K, the effective radiative decay rate is ηw_{obs} , where w_{obs} is the observed decay rate. Within experimental accuracy, we find that $\eta w_{\text{obs}} = w_m$. Thus the effect of increased temperature is to average over the distribution of radiative rates, and simultaneously to permit exciton migration to nonradiative centers, pro-

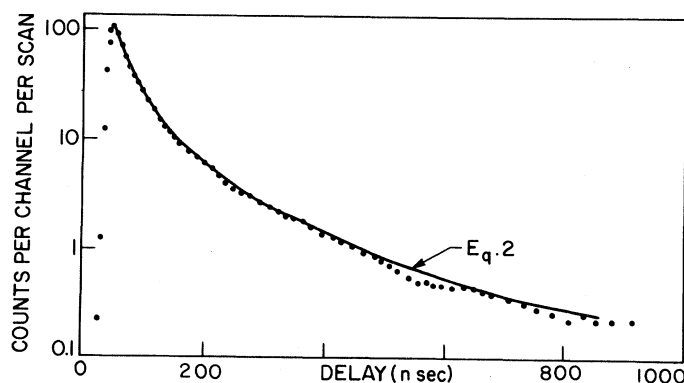


FIG. 6. Luminescent decay curves at 2 K of the no-phonon line for $x=0.46$, excited as in Fig. 5. Gatewidth equals 10 nsec. Points are experimental; the solid line is Eq. (2).

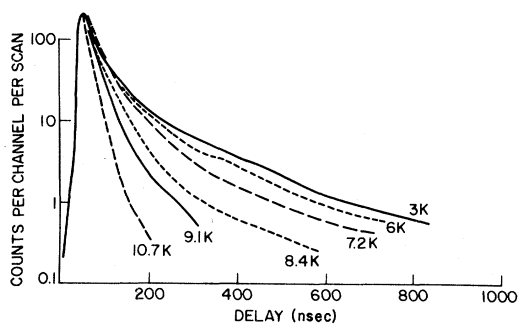


FIG. 7. Temperature dependence of the decay of the no-phonon luminescence for $x=0.46$. Excitation as in Fig. 5.

ducing the drop in efficiency already noted in the cw data. Consistent with this picture, the decrease in efficiency with temperature is much less pronounced at high intensities.

The excitation intensity can be increased in two ways, by lengthening the pulse from the acousto-optically modulated cw laser, or by using the N_2 -pumped dye laser, which gives up to 10^4 times higher peak power. Lengthening the pulse is, of course, only of limited value when the lifetime is short. Some results obtained with a 250-nsec pulse are shown in Fig. 8. Note the changeover from nonexponential to exponential decay, and the large increase in radiative efficiency, as the intensity is increased.

The low repetition rate (50 Hz) of our N_2 -pumped laser precludes the use of intensities sufficiently low

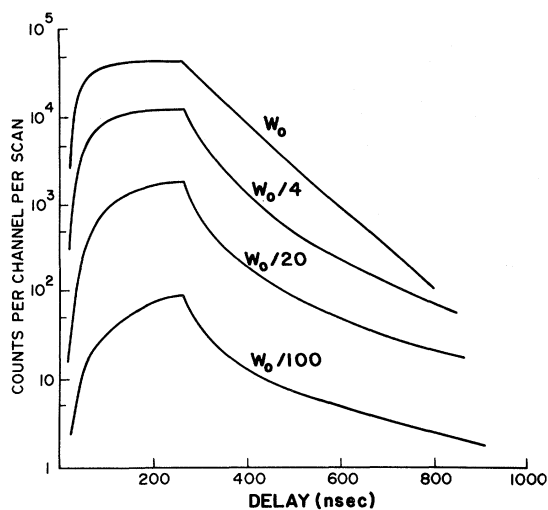


FIG. 8. Time dependence of the no-phonon luminescence at 2 K for $x=0.445$, excited by a 250-nsec pulse of various intensities. $W_0 \sim 10^{20}$ photons $\text{cm}^{-2} \text{sec}^{-1}$ at 5145 Å. Gatewidth is 10 nsec.

to reach the nonexponential regime. It also means that much higher peak powers are required to saturate the nonradiative decay and the DA luminescence. Below the threshold for the creation of an electron-hole plasma, the decay is always exponential, with a lifetime and radiative efficiency which increases with excitation intensity. The limiting (high intensity) value of the exciton decay rate, τ^{-1} , is plotted as a function of x in Fig. 9. Also shown are the fitted values of w_m . These are typically slightly larger than the corresponding exponential decay rates. Figure 9 also shows the exponential decay rates at high intensity in some deliberately doped samples.

The increase in efficiency and lifetime with increasing excitation intensity shows that nonradiative decay paths are becoming saturated. For values of x well away from crossover ($x \geq 0.47$) they never become completely saturated, and the decay remains predominantly nonradiative right up to the plasma threshold. Near crossover (i.e., for $0.435 < x \lesssim 0.46$),

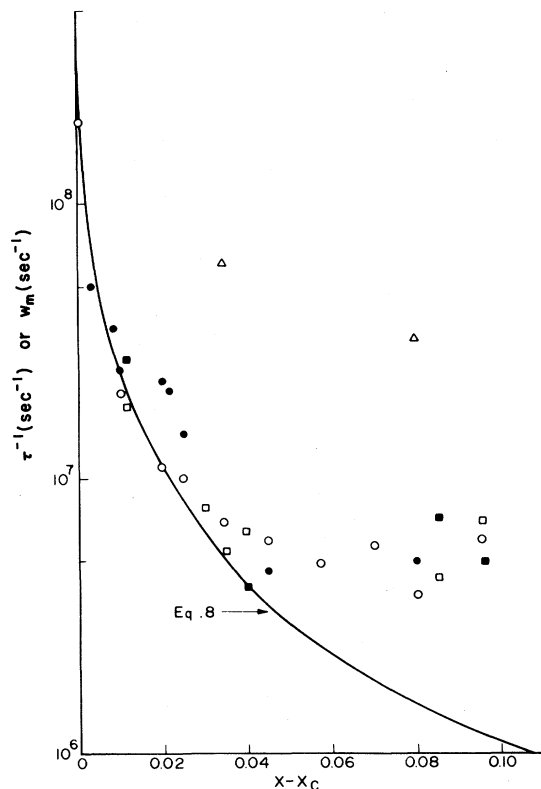


FIG. 9. Observed exponential decay rate at high excitation, τ^{-1} (open symbols), and mean decay rate at low excitation w_m (closed symbols) in $\text{Ga}_{1-x}\text{Al}_x\text{As}$, as a function of x and of doping. Symbols as in Fig. 2. The solid line is Eq. (8), with $w_0 = 4 \times 10^8 \text{ sec}^{-1}$.

however, this is not the case, and decay is primarily radiative at high excitation level. This is shown by the approximate equality of τ^{-1} and w_m , and is confirmed by the fact that the luminescent efficiency shows no appreciable change when plasma emission replaces the exciton emission, even though the decay rate increases by a factor of 5. Even when stimulated emission occurs, and the decay rate increases by at least an order of magnitude, the overall efficiency does not change (although this is difficult to measure accurately, because of the directionality of the stimulated emission). It follows that nonradiative decay does not make an appreciable contribution to the rate, and the luminescent efficiency is close to 100%, so long as the excitation level is high enough.

IV. DISCUSSION

A. Origin of the no-phonon line in undoped samples

The long lifetime and high radiative efficiency found for the indirect exciton show that the emission cannot be assigned to excitons bound to neutral donors, as has been done in the past.^{12,13} (Our samples, being *n*-type, contain no neutral acceptors at low excitation intensity. Ge-doped samples, which are *p* type, show no exciton emission at all.) Excitons bound to Sn or Te donors decay exponentially with lifetimes less than 20 nsec even for $x \geq 0.5$ (see Fig. 9). This is generally true of such three-particle systems, since they can decay rapidly by nonradiative Auger recombination.

As we shall see in Sec. V, excitons bound to the isoelectronic trap N also have a very short lifetime. Very close to crossover Kleiman²¹ predicts subnanosecond radiative lifetimes for excitons bound even weakly to isoelectronic traps, since the lifetime of large bound excitons is greatly shortened by the Rashba ("giant oscillator strength") effect.²²

Further evidence that the emission is not from excitons bound to impurities is provided by the excitation spectrum of the phonon sideband. This spectrum is identical to that of the no-phonon line and shows weak excitation in the indirect gap region, with the spectral dependence predicted for absorption induced by alloy scattering or weak impurity scattering^{2,3,23} [see Eq. (6) below]. Scattering by an impurity potential strong enough to bind an exciton gives a quite different dependence.²⁴ Pumping at the no-phonon line, on the other hand, does *not* excite the sideband (less than 10^{-4} of the maximum excitation efficiency). This is contrary to what one expects for a bound exciton, for which pumping in the no-phonon line should excite the sideband very efficiently.

An alternative explanation, that the emission is

not from excitons at all, but from free-to-bound transitions (i.e., the recombination of a free electron at a neutral acceptor, or a free hole at a neutral donor), can be ruled out by the temperature dependence of the emission. At low excitation the emission falls off rapidly in the (10–20)-K range, with little change in shape. Transitions involving free particles should increase in intensity and broaden, as the temperature is raised and bound states become thermally ionized.

We are left with the only remaining possibility, that the emission is intrinsic, coming from the decay of free excitons moving in the random potential of the alloy. The no-phonon line, strictly forbidden by \vec{k} conservation in a perfect crystal, is allowed by alloy scattering.^{3,16,23} The band gap varies from point to point in the crystal, because of random fluctuations in composition, and free excitons will tend to migrate to regions of lower band gap. This migration will, however, be greatly inhibited by scattering, which will also prevent the excitons migrating freely to impurity and defect centers.

The relation between the data obtained at high and low excitation intensities can be understood qualitatively on the following model. We assume that there is a wide range of exciton mobilities, and that there is no correlation between the energy of the exciton (so long as it is in the low-energy tail, which is the only region which we can observe in luminescence) and its mobility. This second assumption, which is contrary to the usual picture of a "mobility edge" in a disordered medium,²⁵ is essential to account for the fact that the no-phonon spectrum is identical at high and low intensity. It implies that the exciton broadening is predominantly macroscopic; i.e., it is due to band-gap fluctuations on a spatial scale so large that there is no communication between regions of different band gap. Macroscopic broadening will also account for the absence of thermalization of the most mobile excitons. If they could diffuse to regions of low band gap, the bandwidth could not exceed about 3 kT, which is 0.5 meV at 2 K.

Consider first the case of low intensity (impurities all ionized). Excitons are created randomly throughout the crystal. These within a few Bohr radii of an ionized impurity will be immediately destroyed by the associated electric field. However, since the impurity density $N_i \leq 10^{17} \text{ cm}^{-3}$, while $a_B \sim 30 \text{ \AA}$, only a small fraction should be lost in this way. An exciton created elsewhere will radiate if its mobility is so low that it cannot migrate a distance $\sim N_i^{-1/3} \sim 300 \text{ \AA}$ within its radiative lifetime. Excitons that can move this far will be destroyed. Excitons that cannot move very far within their radiative lifetime (i.e., "localized" excitons) will ex-

perience a distribution of Γ - X scattering rates and hence have a distribution of radiative lifetimes¹⁶ (see the next section). Thus these will show nonexponential decay. In order for an exciton to average over this distribution, and show exponential decay, it must, within its lifetime, "visit" $\sim n$ distinct sites, where $n \sim a_B^3/\Omega \sim 300$ (Ω is the atomic volume). If the exciton motion is diffusive, it will have migrated a distance at least $\sim a_B n^{1/2} \sim 500$ Å in the course of these visits; if ballistic, even further. It follows that a mobile exciton (i.e., one which is sufficiently mobile to average the scattering rate) can also reach an ionized impurity and will be destroyed before it decays radiatively. This is why, at low excitation intensities, we see only luminescence from the localized excitons, which decay nonexponentially. Experimentally, these form only a small fraction of the whole.

As the temperature is raised these localized excitons become sufficiently mobile to average out their scattering rate and decay exponentially. They can also reach ionized impurities; thus the radiative efficiency drops off.

The cw data show that the activation energy E_a for this process depends on the exciton energy $h\nu$. If the broadening of the exciton line were entirely due to band-gap fluctuations on the scale of the exciton diffusion length (i.e., microscopic broadening), we would expect $E_a + h\nu = E_m = \text{const}$, where E_m is the energy of the mobility edge, if it exists. In fact $dE_a/d(h\nu) \sim -\frac{1}{2}$, rather than -1 implying that about half the observed exciton linewidth is due to macroscopic broadening.

At high excitation intensity all the ionized impurities become neutralized and are no longer capable of destroying an exciton. All excitons can now decay radiatively, and, since the majority are mobile, we see a predominantly exponential decay. This picture ignores unsaturable traps, such as deep recombination centers which are strongly coupled to the lattice, and it also ignores Auger decay of excitons in the vicinity of neutral impurities.²⁶ When the radiative lifetime is sufficiently long, these nonradiative processes will dominate the lifetime of mobile excitons. This is presumably the reason why, for $x - x_c \geq 0.05$, τ^{-1} (measured at high intensities) levels off at about $5 \times 10^6 \text{ sec}^{-1}$. The increase in luminescent efficiency with excitation also becomes less pronounced.

The changeover from nonexponential to exponential decay as the excitation intensity is increased is accompanied by the disappearance of the phonon sidebands. This is the expected result of changeover from localized excitons, which can couple strongly to the lattice, to delocalized ones, which cannot.²⁷ To our knowledge this changeover has not previous-

ly been observed.

At low intensities, in the nonexponential regime, the fitted value of w_m does not vary as rapidly with x as expected. Moreover the decay, while still nonexponential, ceases to follow Eq. (2) for $x \gtrsim 0.48$. Probably tunneling to nonradiative centers is becoming important. The distribution of tunneling rates will lead to nonexponential decay which, however, has a very different form from Eqs. (2) or (3).²⁸

B. Theory of the radiative decay rate

Faulkner²⁴ has calculated the transition probability for the creation of indirect excitons in the presence of a short-range potential which scatters electrons from X to Γ . He finds a very complex dependence of absorption on energy, which can, however, be greatly simplified when the scattering is weak, so that the Born approximation can be used. In this approximation the electron wave function is given by

$$\psi_e = \psi_X + \frac{J\Omega}{(2\pi)^3} (E - \Delta)^{-1} \psi_\Gamma, \quad (4)$$

where J is the scattering matrix element defined in Faulkner's equation (3.2): E is the electron energy measured from the indirect band edge E_X , and $\Delta = E_\Gamma - E_X$, where E_Γ is the direct band gap. Faulkner's equation (3.58) for the absorption coefficient $\alpha(\hbar\omega)$, due to the creation of free excitons, becomes in this approximation

$$\alpha(\hbar\omega) = \alpha_0 \left[\frac{E_\Gamma}{\Delta - E} \right]^2 \left[\frac{\epsilon}{\epsilon_X} \right]^{1/2} \left[1 + \frac{\epsilon}{\epsilon_X} \right], \quad (5a)$$

where

$$\alpha_0 = \frac{3.2^6}{\pi n_R \hbar\omega} \frac{e^2}{\hbar c} |P_\Gamma|^2 \Omega^2 \left[\frac{m_e m_h}{\hbar^4} \right]^{3/2} \epsilon_X^2 J^2 N_s. \quad (5b)$$

Here n_R is the refractive index, P_Γ the optical matrix element at Γ , m_e and m_h the electron and hole masses, ϵ_X the binding energy of the indirect exciton, $\epsilon = E + \epsilon_X$, $\hbar\omega = E + E_X$, and N_s is the number of scattering centers per unit volume. Note that Eq. (5b) has been corrected by a factor \hbar^{-6} , which Faulkner omitted.

Equation (5) diverges for $\Delta = E$. This is a consequence of Faulkner's neglect of $k \neq 0$ contributions to α (an approximation which is fully justified for the case which he was considering, GaP:N, where $\Delta \sim 0.5$ eV). Kleiman²³ has repeated Faulkner's calculation for the *bound* exciton, including $k \neq 0$ contributions, and finds that the factor $(\Delta - E)^{-2}$ must

be replaced by $[\epsilon_\Gamma^{1/2} + (\Delta - E)^{1/2}]^{-4}$, where ϵ_Γ is the binding energy of the free direct exciton. Making the same substitution for the free-exciton case, we replace Eq. (5) by

$$\alpha = \alpha_0 \left[\frac{E_\Gamma}{\epsilon_\Gamma} \right]^2 \left[1 + \left[\frac{\Delta - E}{\epsilon_\Gamma} \right]^{1/2} \right]^{-4} \times \left[\frac{\epsilon}{\epsilon_x} \right]^{1/2} \left[1 + \frac{\epsilon}{\epsilon_x} \right]. \quad (6)$$

The mean radiative decay rate w_m can be obtained from α through the Einstein relations. At $T=0$, for an isotropic medium, these give²⁹

$$w_m = \frac{\hbar}{\tau_R} = \hbar \left[\frac{n_R \omega}{\pi c} \right]^2 \lim_{\epsilon \rightarrow 0} \frac{\alpha(\epsilon)}{g(\epsilon)}, \quad (7)$$

where $g(\epsilon)$ is the exciton density of states. Hence

$$w_m = w_0 [1 + (\Delta/\epsilon_\Gamma)^{1/2}]^4, \quad (8a)$$

where

$$w_0 = \frac{36}{\pi} \left[\frac{e^2}{\hbar c} \right] n_R \omega^3 c^{-2} \left[\frac{E_\Gamma}{\hbar \omega} \right]^2 \left[\frac{2\mu\epsilon_x}{\hbar^2} \right]^{3/2} \times \Omega |P_\Gamma|^2 \left[\frac{J}{\epsilon_\Gamma} \right]^2 \Omega N_s, \quad (8b)$$

and $\mu = m_e m_h / (m_e + m_h)$ is the reduced mass of the indirect exciton. Substituting $\epsilon_x = 20$ meV, $\mu = 0.2m_0$, $|P_\Gamma| = 4$ Å (the value obtained for GaP:N by Faulkner,²⁴ corrected for the erroneous calibration of nitrogen content which he used), we obtain (in sec^{-1})

$$w_0 \sim 3 \times 10^6 \left[\frac{J}{\epsilon_\Gamma} \right]^2 \Omega N_s. \quad (9)$$

For alloy disorder scattering, in which essentially every atom scatters, we should substitute $x(1-x)$ for (ΩN_s) (Refs. 16 and 23) and define J as the difference between the scattering matrix elements of Al and Ga ($V_{\text{Al}} - V_{\text{Ga}}$ in the notation of Ref. 16).

The solid curve in Fig. 9 is obtained from Eq. (8), with $\epsilon_\Gamma = 8$ meV (Ref. 30) and $w_0 = 5 \times 10^8 \text{ sec}^{-1}$. This fitted value of w_0 confirms that the scattering is intrinsic, i.e., alloy scattering, rather than extrinsic, from impurities or defects. If we substitute w_0 in Eq. (9), and we find $J(\Omega N_s)^{1/2} = 0.1$ eV. It is known from Faulkner's work that if $J \geq 2$ eV, the Born approximation breaks down and a bound-state exists, as in GaP:N. This is not observed; hence $J \lesssim 2$ eV, and $(\Omega N_s)^{1/2} \geq 0.05$, or $N_s \geq 10^{19}$. This is 2 orders of magnitude greater than the impurity content of our samples. Hence the scattering must be intrinsic, and we have (since $x \approx 0.5$)

$J = |V_{\text{Al}} - V_{\text{Ga}}| \approx 0.2$ eV, or 0.1 of the value for N in GaP.

According to Phillips,³¹ the electronegativity difference between N and P in GaP is 1.36 eV, while that for Al and Ga in GaAs is 0.05 eV. Pauling's³² values are 0.9 and 0.1 eV, respectively. Thus it appears that J scales roughly as the electronegativity (insofar as it can be accurately defined for an impurity atom), in agreement with Hopfield's original theory of the isoelectronic trap.³³

So far we have only considered the *average* value of the exciton decay rate. In fact, as we have seen, the decay at low temperature and excitation level is nonexponential, and does not have a well-defined rate constant. It has been pointed out by Klein *et al.*¹⁶ that the strength of Γ -X scattering due to alloy disorder, i.e., the value of $|J|^2$ when averaged over the exciton volume, has an exponential probability distribution:

$$p(|J|^2) = \langle J^2 \rangle^{-1} \exp(-|J|^2 / \langle J^2 \rangle). \quad (10)$$

This follows directly from the fact that J is a stochastic complex variable. For localized excitons we would therefore expect a corresponding distribution of radiative decay rates w . There will also be a contribution to the exciton decay rate from momentum-conserving (MC) phonon-assisted processes and from nonradiative decay; we will neglect any variance in this rate and call it w_1 . Then the intensity of the no-phonon line at time t after pulsed excitation will be

$$I_{\text{np}}(t) = N_1 \int_0^\infty w e^{-(w+w_1)t} p(w) dw \quad (11)$$

$$= \frac{N_1 w_m e^{-w_1 t}}{(1+w_m t)^2}, \quad (2')$$

where N_1 is the number of excitons created initially and w_m is the mean value of w . Similarly the intensity of the sideband due to MC phonons alone will be

$$I_{\text{sb}}(t) = N_1 w_s \int_0^\infty e^{-(w+w_1)t} p(w) dw \quad (12)$$

$$= \frac{N_1 w_s e^{-w_1 t}}{1+w_m t}, \quad (3')$$

where w_s the radiative rate for the MC process. It was shown in the preceding section that Eq. (2) fits the data well, and the resulting values of w_m were shown as a function of x in Fig. 9.

V. EFFECT OF NITROGEN DOPING

Although many samples were grown in an ambient containing NH_3 , the effect on the spectrum was found usually to be minimal. There is a slight downwards shift (~ 2 meV) in the position of the

no-phonon line, a significant enhancement of the strength of the phonon sidebands, and a slight increase in the radiative efficiency and in the absorption in the indirect-gap region, as detected in the luminescence excitation spectrum. As in undoped material, pumping at the energy of the no-phonon emission line does not excite the phonon sideband: Hence the exciton is not bound to the nitrogen impurity.

One sample, however, with $x=0.52$, showed quite different behavior. Figure 10 shows the photoluminescence spectra of this crystal, excited with a cw laser at 2.082 eV, taken at 2 and 4.2 K. The 2-K spectrum is similar to that shown in Fig. 1(b) for the lightly N-doped sample with the same x (same peak positions for the no-phonon line and phonon sidebands). However, while there is virtually no change with temperature in the peak energies for other samples between 2 and 15 K, a marked change is observed for this more heavily doped sample: Upon raising the temperature to 4.2 K the no-phonon line and phonon sidebands shift by 9 ± 1 meV towards the red. The position of the new line, designated N_1 in Fig. 10, agrees with that observed in $\text{Ga}_{1-x}\text{Al}_x\text{As}$ doped with nitrogen by ion implantation.^{10,11} The luminescence obtained with selective high-level excitation of the N_1 band decays exponentially with a lifetime of about 10 nsec at 4.2 K, as compared with the 200-nsec lifetime obtained with intense above-band-gap excitation which saturates the N_1 luminescence. (Low-level measurements of lifetime were not made on this sample.)

The line designated N_1 is actually the strongest and highest energy component of a broad band spreading from 2.052 eV down to about 2.00 eV,

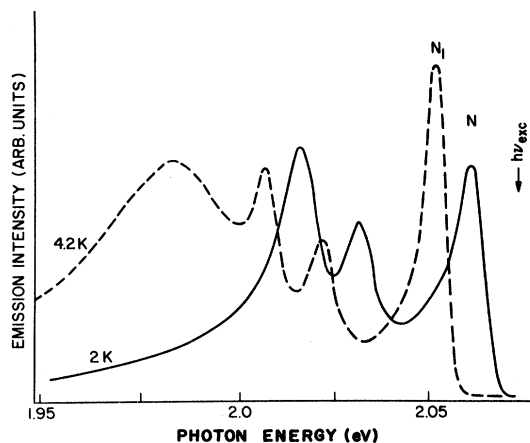


FIG. 10. Luminescence at 2 and 4.2 K of $\text{Ga}_{0.48}\text{Al}_{0.52}\text{As:N}$, excited just below the direct band gap (cw excitation).

which can be seen as a broad background in Fig. 10 ($T=2$ K). Its lowest edge is difficult to determine as it overlaps with the DA pair spectrum. Various components of this band can be selectively excited, as shown in Fig. 11(a). Optical-phonon sidebands are absent in all the spectra taken with excitation energy lower than 2.06 eV (the peak designated N in Fig. 10 is the only no-phonon line observed in the other nitrogen-doped samples). Since this emission comes from localized exciton states, we might have expected LO-phonon sidebands as in the case of the localized intrinsic exciton. However, if the $X-\Gamma$ mixing by the impurity potential is strong, as it is for the nitrogen-bound exciton in GaP, and as it must be to produce the short lifetime observed, the no-phonon line will dominate the spectrum and the MC phonon sidebands will be too weak to see. All the spectral components shown in Fig. 11(a) have a 10-nsec lifetime and all have much the same intensity when selectively excited. Figure 11(b) shows the excitation spectra of various components of the N_1 band (monitored with a resolution of 0.3 meV). All these excitation spectra show a peak 3–6 meV above the monitored energy, the smaller separation corresponding to the lower emission energy. Note that the N band, at 2.062 eV, does not appear in the excitation spectrum of that part of the N_1 band below about 2.05 eV. The excitation spectrum above 2.06

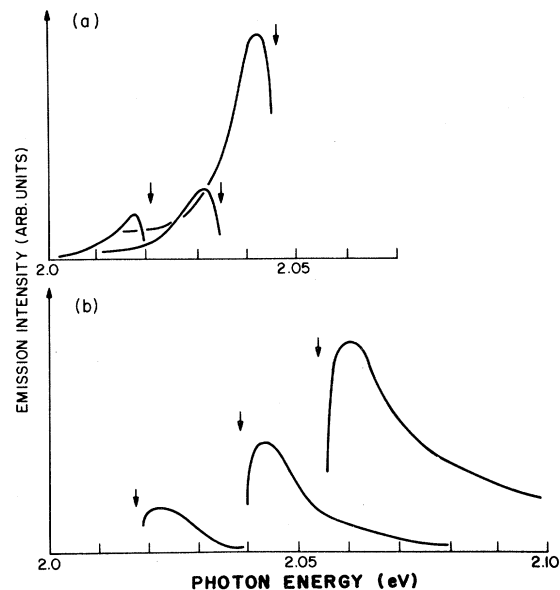


FIG. 11. Selectively excited luminescence at 4.4 K in $\text{Ga}_{0.48}\text{Al}_{0.52}\text{As:N}$. (a) Emission excited by fixed cw laser frequencies (indicated by arrows) within the nitrogen bound exciton band N_1 . (b) Excitation spectra for different monitored emission frequencies (arrows) within regions of the N_1 band.

eV is similar to that reported by Makita and Goude,^{10,34} who did not, however, observe the excitation at lower energies which is reported here.

The fact that emission can be excited by radiation in the entire range from 2.0 to 2.05 eV shows that there is a broad band of bound-exciton states associated with nitrogen impurities. The width is comparable with that of the corresponding band in Ga(As,P):N,¹³ although the binding energy is somewhat less and the excitation behavior quite different. The great width of the nitrogen bound-exciton band, N_1 , as compared with the donor-bound and "intrinsic" excitons described previously, is presumably due to the short-range nature of the binding to an isoelectronic trap such as nitrogen. Since the binding potential is more or less localized on a single impurity atom, its strength is strongly dependent on the few nearest neighbors and is therefore subject to strong fluctuations.

The simplest interpretation of the excitation spectrum is that the N_1 nitrogen bound-exciton state is split by about 5 meV.³⁵ This splitting is inhomogeneously broadened by about 2 meV, and is negatively correlated with the binding energy, so that the more strongly bound the exciton, the smaller the splitting. Exchange splitting is expected to be ~ 1 meV and to increase with binding energy. The natural explanation of the observed splitting is that there is an axial "crystal field" at the nitrogen site. Such a crystal field would arise, for example from the random distribution of Al and Ga over near neighbor sites. It has been invoked to account for the depolarization and anomalous x dependence of excitons in CdS _{x} Se _{$1-x$} .³⁶

The spectra reported in Refs. 10 and 11 (in which the samples were heavily doped by ion implantation) shows this N_1 band as the most prominent spectral feature. These authors also observed two additional bands (designated N_2 and N_3 in Ref. 10) which they also associate with nitrogen. We find that these bands are indistinguishable from the donor-acceptor pair bands and we believe that their association with N is doubtful. Wolford *et al.*¹¹ identify these bands as multiple LO-phonon sidebands of the N_1 band. However, the selectively excited spectra presented in Fig. 11(a) clearly show that coupling to LO phonons is virtually nonexistent. Furthermore, we found that N_2 and N_3 , unlike N_1 , could not be excited selectively.

We turn now to the remarkable temperature dependence illustrated in Fig. 10. These data give a very clear indication of thermally activated energy transfer, as can be seen as follows: At most of the sites which are influenced by the nitrogen doping, the effect on the exciton is slight. These sites give rise to the N band, whose emission is almost identi-

cal to that of the localized intrinsic exciton in undoped material. Band-gap excitation populates these states predominantly. At 2 K excitons are localized on these sites long enough to decay radiatively. When the temperature is raised they can diffuse by thermally activated hopping and can be captured by the slightly deeper N_1 type of site. The capture process is preferential: Only those N_1 sites which emit about 6 meV below the N band are populated by N or band-gap excitation. This can be understood if the N_1 bound-exciton level is split, since resonant transfer can occur into the excited state, followed by rapid phonon-assisted thermalization into the "ground" emitting state.

VI. CONCLUSIONS

We have shown that the indirect exciton non-phonon emission near crossover in LPE Ga _{$1-x$} Al _{x} As is intrinsic. It comes from the recombination of free excitons scattered by the random alloy potential, rather than from excitons bound to impurities, as was previously thought. The average value of the Γ - X scattering matrix element J is 0.2 eV, within a factor of 2 of that predicted by naive electronegativity arguments.

A small fraction of the excitons are sufficiently localized, on the timescale of the radiative lifetime, that they can see the fluctuations in the Γ - X scattering potential and decay nonexponentially. Their migration is thermally activated, but whether they are localized, in the Anderson sense, at 0 K remains to be established.

The majority of excitons can migrate far enough within their lifetime to average out the Γ - X scattering and therefore decay exponentially. Since these excitons can reach nonradiative centers such as ionized impurities, they only radiate at high excitation level, where the nonradiative centers are saturated. Furthermore, since these excitons have the same spectral distribution as the "localized" ones, and do not thermalize, much of the exciton linewidth of about 6 meV must come from macroscopic broadening. The exciton bound to nitrogen is split by more than just exchange. This may be due to a local disorder-induced axial field.

ACKNOWLEDGMENTS

We are grateful to M. V. Klein for communicating his unpublished work, and for helpful discussions, and to R. C. Dunne and H. G. White for technical assistance. Part of this work was done at the Physics Department and Solid State Institute, Technion, Haifa, Israel, where it was supported in part by the U.S.—Israel Binational Foundation.

- *Permanent address: Physics Department and Solid State Institute Technion, Haifa, Israel.
- ¹P. J. Dean and D. C. Herbert, in *Excitons*, edited by K. Cho (Springer, Berlin, 1979), p. 55.
 - ²A. N. Pikhtin, *Fiz. Tekh. Poluprovodn.* **11**, 425 (1977) [*Sov. Phys.—Semicond.* **11**, 245 (1977)].
 - ³S. D. Baranovskii and A. L. Efros, *Fiz. Tech. Poluprovodn.* **12**, 2233 (1978) [*Sov. Phys.—Semicond.* **12**, 1328 (1978)].
 - ⁴P. J. Dean, G. Kaminsky, and R. B. Zetterstrom, *Phys. Rev.* **181**, 1149 (1969); P. J. Dean, *J. Lumin.* **1-2**, 398 (1970).
 - ⁵S. Lai and M. V. Klein, *Phys. Rev. Lett.* **44**, 1087 (1980).
 - ⁶M. G. Craford and N. Holonyak, Jr., in *Optical Properties of Solids: New Developments*, edited by B. O. Seraphin (North-Holland, Amsterdam, 1976), p. 187; R. J. Nelson, N. Holonyak, Jr., J. J. Coleman, D. Lazarus, W. O. Groves, D. L. Keune, M. G. Craford, D. J. Wolford, and B. G. Streetman, *Phys. Rev. B* **14**, 685 (1976).
 - ⁷D. M. Roessler and D. E. Swets, *J. Appl. Phys.* **49**, 804 (1978); J. Chevallier, H. Mariette, D. Diguët, and G. Poiblaud, *Appl. Phys. Lett.* **28**, 375 (1976).
 - ⁸R. J. Nelson and N. Holonyak, Jr., *J. Phys. Chem. Solids* **37**, 629 (1976).
 - ⁹H. Mariette and J. Chevallier, *J. Appl. Phys.* **48**, 1202 (1977).
 - ¹⁰S. Goude, Y. Makita, S. Mukai, T. Tsurushima, and H. Tanone, *Appl. Phys. Lett.* **29**, 196 (1976); Y. Makita and S. Goude, *J. Appl. Phys.* **48**, 1628 (1977).
 - ¹¹D. Wolford, W. Y. Hsu, J. D. Dow, and B. G. Streetman, *J. Lumin.* **18/19**, 863 (1979).
 - ¹²R. Dingle, R. A. Logan, and R. J. Nelson, *Solid State Commun.* **24**, 171 (1979).
 - ¹³For reviews, see Ref. 2 and R. J. Nelson, in *Excitons*, edited by E. Rashba and M. D. Sturge (North-Holland, Amsterdam, 1982), p. 319.
 - ¹⁴R. Dingle, R. A. Logan, and J. R. Arthur, Jr., in *GaAs and Related Compounds*, edited by C. Hilsum (Institute of Physics, London, 1977), p. 210.
 - ¹⁵E. Cohen, M. D. Sturge, M. A. Olmstead, and R. A. Logan, *Phys. Rev. B* **22**, 771 (1980).
 - ¹⁶M. V. Klein, M. D. Sturge, and E. Cohen, *Phys. Rev. B* **25**, 4331 (1982).
 - ¹⁷W. W. Rigrod, J. H. Mcfee, M. A. Pollack, and R. A. Logan, *J. Opt. Soc. Amer.* **65**, 46 (1975); R. C. Dunne and M. D. Sturge (unpublished).
 - ¹⁸M. Ilegems and G. L. Pearson, *Phys. Rev. B* **1**, 1576 (1970); A. S. Barker and A. J. Sievers, *Rev. Mod. Phys.* **47**, 51 (1975); B. Jusserand and J. Sapriel, *Phys. Rev. B* **24**, 7194 (1981).
 - ¹⁹M. D. Sturge, E. Cohen, and K. F. Rodgers, *Phys. Rev. B* **15**, 3169 (1977).
 - ²⁰P. J. Dean and D. G. Thomas, *Phys. Rev.* **150**, 690 (1966).
 - ²¹G. G. Kleiman, *J. Appl. Phys.* **47**, 180 (1976).
 - ²²E. I. Rashba and G. E. Gurgenishvili, *Fiz. Tverd. Tela (Leningrad)* **4**, 1029 (1962) [*Sov. Phys.—Solid State* **4**, 759 (1962)].
 - ²³A. Baldereschi, E. Hess, K. Macheke, H. Neumann, K.-R. Schulze, and K. Unger, *J. Phys. C* **10**, 4709 (1977).
 - ²⁴R. A. Faulkner, *Phys. Rev.* **173**, 991 (1968).
 - ²⁵N. F. Mott and E. A. Davis, *Electronic Processes in Non-Crystalline Materials* (Clarendon, Oxford, 1979).
 - ²⁶H. J. Queisser, *Solid State Electronics* **21**, 1495 (1978); P. J. Dean and D. C. Herbert, in *Excitons*, edited by K. Cho (Springer, Berlin, 1979), Chap. 3.
 - ²⁷P. W. Anderson, *Nature (Phys. Sci.)* **235**, 163 (1972); Y. Toyozawa, *J. Lumin.* **24/25**, 23 (1981).
 - ²⁸M. Inokuti and F. Hirayama, *J. Chem. Phys.* **43**, 1978 (1965).
 - ²⁹F. Stern, in *Advances in Solid State Physics*, edited by F. Seitz and D. Turnbull (Academic, New York, 1965), Vol. 15, p. 300.
 - ³⁰M. Panish and H. C. Casey, *Heterojunction Lasers* (Academic, New York, 1978).
 - ³¹J. C. Phillips, *Bonds and Bands in Semiconductors* (Academic, New York, 1973), p. 54.
 - ³²L. Pauling, *The Nature of the Chemical Bond* (Cornell University Press, Ithaca, 1960).
 - ³³J. J. Hopfield, D. G. Thomas, and R. T. Lynch, *Phys. Rev. Lett.* **17**, 312 (1966).
 - ³⁴The feature at 2.16 eV in the excitation spectrum, reported in Ref. 10, appears to be associated with excitation of the overlapping DA pair band, not the N_1 band.
 - ³⁵A similar splitting, called there an "exchange" splitting, has been reported in both $Al_xGa_{1-x}As$ and GaP_xAs_{1-x} by D. J. Wolford, M. B. Small, and J. Thompson, *Bull. Am. Phys. Soc.* **26**, 286 (1981).
 - ³⁶O. Goede, D. Hennig, and L. John, *Phys. Status Solidi D* **96**, 671 (1979).